Progress In Electromagnetics Research, Vol. 119, 19–33, 2011

DESIGN OF COMPACT QUADRUPLEXER BASED ON DEFECTED STEPPED IMPEDANCE RESONATORS

J.-Z. Chen*, N. Wang, K. Deng, and S. Yang

School of Electronic Engineering, Xidian University, Xi'an, Shaanxi 710071, People's Republic of China

Abstract—A novel compact quadruplexer based on defected stepped impedance resonator (DSIR) with high isolation is presented in this paper. The proposed quadruplexer consists of a common input feeding line, four kinds of folded DSIRs and four individual output feeding lines. Considering the loading effect among channel filters, the input DSIRs must be properly located with respect to the common feeding line in order to realize all external quality factors at the same time, so that the loading effect becomes very small. Furthermore, since the compact DSIRs resonate at multiple fundamental frequencies, a high-isolation quadruplexer with size reduction can be obtained. A fabricated prototype of the proposed quadruplexer is developed. The channel performance obtained by measurement and EM simulation are in good agreement.

1. INTRODUCTION

In recent years, the rapid progress in mobile and wireless communication technology has increased the need of integrating more than one communication standard into a single system [1, 2], where different standards may use different frequency bands. In these communication systems, the multiplexers are an essential component for channel separation in microwave front-end systems. Recently, much research has been focused on developing various kinds of multiplexers [3–19].

In [3], the authors demonstrated a novel high-isolation multiplexer utilizing high-order parallel-coupled bandpass filters (BPFs) and ring manifold resulting in a large circuit size. In [4], the authors presented

Received 13 June 2011, Accepted 11 July 2011, Scheduled 19 July 2011

* Corresponding author: Jian-Zhong Chen (jianzhongster@gmail.com).

a triplexer with high isolation at the cost of increasing circuit size due to the additional matching network based on the stepped-impedance resonators. In [5], novel microstrip line resonators were proposed to design a microstrip diplexer. Those novel resonators can be used to control the characteristic of the diplexers but with the penalty of additional loaded elements. The ridge waveguide T-junctions were developed for wideband diplexer applications [6, 7]. However, such a waveguide configuration is hard to be integrated directly within a planar system. In a previous work [8], a wide stopband diplexer using the microstrip electromagnetic band gap structure was designed and implemented, but the selectivity is not good. In order to achieve the high isolation and a wide and deep stopband simultaneously, novel microstrip diplexers/filters based on modified stepped impedance resonators(SIR) [9–12], defected ground structure (DGS) [13, 14] and dual mode SIRs [15] were developed and proposed. In addition, two hairpin line filtering structures were proposed to form a diplexer, and a tapped open stub was used to introduce an attenuation pole to suppress the spurious response and achieve a high isolation between two bands [16]. To render further miniaturization of the effective circuit area, the common-resonator configuration was proposed [17–19]. In this configuration, each BPF shares a common resonator. However, the passband frequencies have to be designed at the resonant frequencies of the common resonator, and the freedom in choosing passband frequencies are limited. Furthermore, this type of multiplexers only allows a small number of passbands to be implemented due to the limited coupling area available.

In this study, a quadruplexer with compact size, high isolation, and flexible passband frequencies is presented. Since there are no extra matching networks, the proposed quadruplexer is compact. By properly locating defected stepped impedance resonators (DSIRs) with respect to the distributed common input coupling feeding line, the loading effect among channels will be very small. In addition, because the proposed quadruplexer utilizes the distributed coupling technique instead of a common resonator, the proposed configuration has a high freedom in choosing passband frequencies.

2. RESONANCE PROPERTY OF THE DSIR

The configuration of the proposed folded DSIR is shown in Figure 1. The substrate used in this study has a relative dielectric constant of 2.65, a thickness of 1 mm and a loss tangent of 0.004. The thickness of the metal is 0.035 mm. The DSIR may be thought of as a folded slot line and has opposite impedance characteristic to the

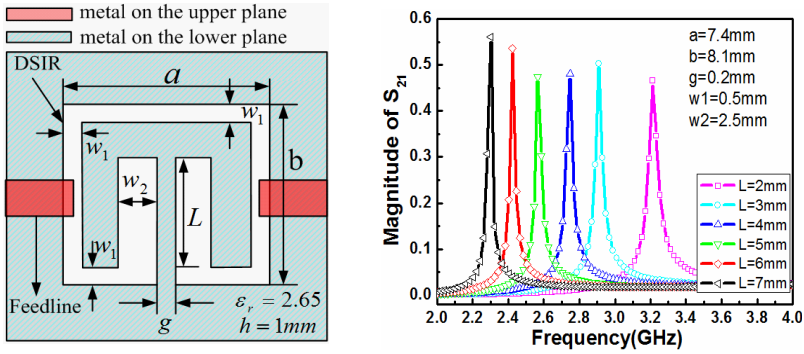

Figure 1. Proposed DSIR. (a) Structure of the DSIR. (b) Resonant property of the DSIR.

microstrip stepped impedance resonators (SIR), which means a narrow gap width ($w1$, $w2$) results in a lower impedance, while a wide gap width results in a higher impedance. So the impedance ratio of the DSIR is approximately equivalent to $K_{\mathrm{DSIR}} \approx 1/K_{\mathrm{SIR}}$. To observe the property of the proposed structure, we perform the full-wave EM simulation by computing the transmission response of a single DSIR fed by microstrip lines. The folded DSIR has a structure dimension as follows: $a = 12\,\mathrm{mm}$, $b = 8.1\,\mathrm{mm}$, $g = 0.2\,\mathrm{mm}$, $w1 = 1.1\,\mathrm{mm}$, $w2 = 1.8\,\mathrm{mm}$. Both the input and output terminals have a line width of 3.3 mm and there is an overlapped part to achieve weak external coupling. From Figure 1(b) we find that, a resonant peak appears at about 2.45 GHz, which moves to higher frequency when the length L of the loaded stub decreases. If $L = 0$, the resonator becomes a uniform impedance resonator. The magnitude of the peak mainly depends on the external coupling strength. The DSIR can be utilized to build up compact multiplexers as presented in this study.

3. DESIGN OF A QUADRUPLEXER BASED ON DSIRS

Figure 2 shows the typical coupling structure of the proposed quadruplexer in this study, which is composed of a common input feeding line (port 1), four kinds of resonators (Ra1 to Rd4), and four individual output feeding lines (port 2 to port 5). The presented quadruplexer is formed by combining a fourth-order cross-coupled BPF (0.1 dB ripple level) and three fourth-order Chebyshev BPFs (0.1 dB ripple level) together. The center frequencies of the four

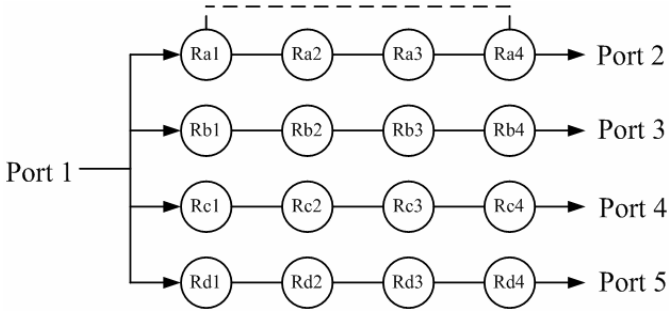

Figure 2. Typical coupling schemes of the proposed quadruplexer. The node denotes a DSIR, the solid line denotes direct coupling between DSIRs and the dashed line denotes the cross coupling between DSIRs.

Table 1. Coupling coefficients and external quality factors.

channels	$F0$ (GHz)	FBW	Qe	$K12/K34$	$K23$	$K14$
1	2.45	6.5%	14.803	0.0561	0.0495	−0.0111
2	3.50	7.0%	13.442	0.0632	0.0486	0
3	4.20	6.6%	14.049	0.0605	0.0465	0
4	5.25	7.5%	12.372	0.0687	0.0528	0

channels are 2.45, 3.50, 4.20 and 5.25 GHz respectively, and the fractional bandwidths are 6.5%, 7.0%, 6.6% and 7.5% respectively. The coupling coefficients and external quality factors corresponding to the specifications from the optimization method in [20] are shown in Table 1. It is worth noting that the filters for each channel are independently synthesized, and an additional complicated optimization step of the complete quadruplexer is not required.

The design starts with choosing dimensions for DSIRs operating at the center frequencies of the four channel filters (BPF1–BPF4). The dimensions of the four kinds of the DSIRs can be easily obtained by using the method described in Section 2. Table 2 shows the physical sizes of the four kinds of DSIRs.

As known to all, when several filters are connected together to a common input feeding line, interaction is inevitable, which will result in degradation of the transfer characteristics of the individual filters. It is worth noting that, when the defected resonators were used to generate a notched band in ultra-wideband BPFs, these defected structures on the ground plane have wake influence on the band characteristics of the filters, as described in literatures [21–23]. Benefitting from this physical

Table 2. Dimensions (in mm) of each part of the DSIRs used in the four channels.

	a	b	g	$W1$	$W2$	L
Ra1–Ra4	7.4	8.1	0.2	0.5	2.5	5.55
Rc1–Rc4	5.4	5.9	0.4	0.5	1.5	1.9
	a	b	g	$W1$	$W2$	L
Rb1–Rb4	7.4	6.15	0.4	0.5	1.5	2.6
Rd1–Rd4	5.4	4.3	0.4	0.5	0.5	2.15

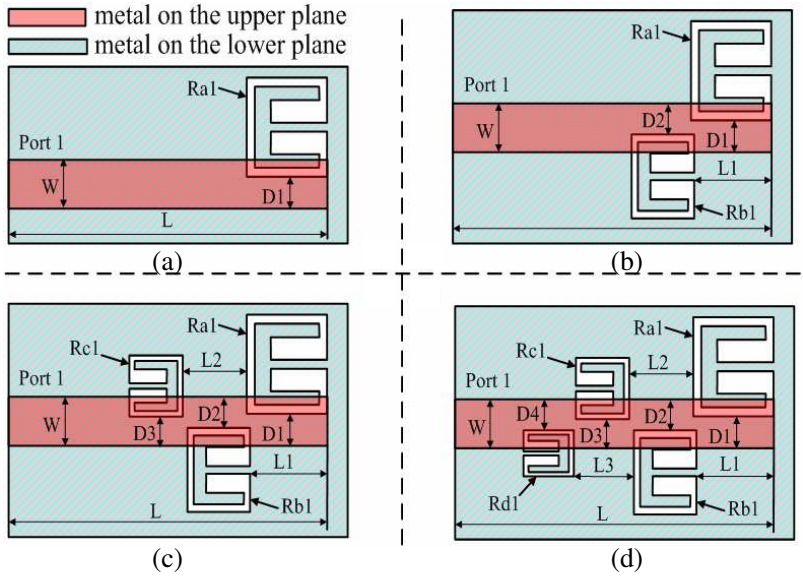

Figure 3. Design procedure of the input coupling structure with DSIRs. (a) Design of the first channel input $Qe1$. (b) Design of the second channel input $Qe2$. (c) Design of the third channel input $Qe3$. (d) Design of the fourth channel input $Qe4$.

phenomenon, loading effects among different resonance DSIRs may be small when the DSIRs were used to design a quadruplexer as long as they are fixed in proper position. In our study, the input external quality factors of the four channels can be satisfied simultaneously so that the loading effect problem is relieved. The input external quality factors ($Qe1$, $Qe2$, $Qe3$, and $Qe4$) between the resonators (Ra1, Rb1, Rc1, Rd1) and the common feeding line will be determined step by step

in this paper. The design procedure of the input coupling structure is illustrated in Figure 3. The width and length of the input common feeding line were selected as 3.3 mm and 31.85 mm. Figure 3(a) depicts the input external coupling structure of the first DSIR (Ra1) with an overlapped feeding line. The feeding line is parallel to the split-ring edge of the input resonator and has a displacement of $D1$. The external quality factor can be obtained by the equation written as follows [24],

$$Q_e = \frac{f_0}{\Delta f_{\pm 90^\circ}} \tag{1}$$

where f_0 is the resonant frequency and can be determined from the peak of the group delay response. $\Delta f_{\pm 90^\circ}$ is the frequency difference between the two frequencies, the phase of which shifts $\pm 90^\circ$ with respect to the phase of resonant frequency from the phase response.

The external quality factor of the first channel ($Qe1$) which are

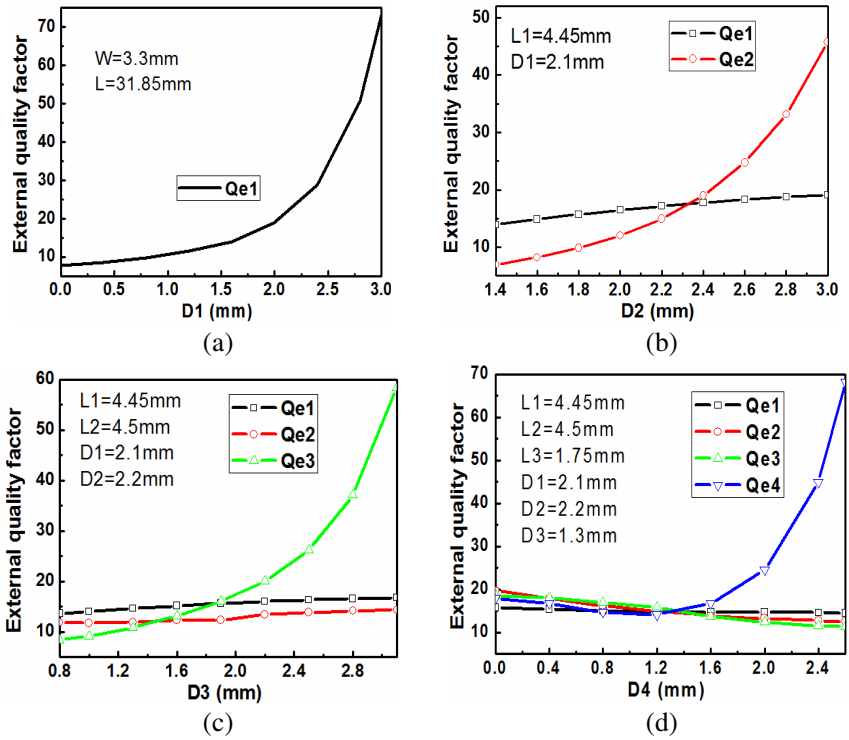

Figure 4. Extracted input external quality factors with respect to the corresponding physical parameters. (a) $Qe1$. (b) $Qe1$ and $Qe2$. (c) $Qe1$, $Qe2$ and $Qe3$. (d) $Qe1$, $Qe2$, $Qe3$ and $Qe4$.

extracted from simulation varied with different inserted distance $D1$ are shown in Figure 4(a). According to the given external quality factor, the initial displacement $D1$ of the parallel feeding line to DSIR ring can be selected from Figure 4(a). After the Ra1 has been fixed in the suitable position of the feeding line, a particular place can be easily found to set the input DSIR (Rb1) of the second channel to achieve the required input external couplings of both existing channels as depicted in Figure 3(b). Figure 4(b) shows the variation of extracted $Qe1$ and $Qe2$ with respect to distance $D2$ when $L1 = 4.45\,\text{mm}$ and $D1 = 2.1\,\text{mm}$. It can be found from Figure 4(b) that the input Rb1 of the second channel has weak affection on $Qe1$ of the first channel. Thus, this new configuration method is able to ensure minimal interaction between the individual channels. Similarly, Rc1 and Rd1 were located as shown in Figures 3(c)–(d) after the DSIR of the previous channel has been posited. It can be verified again from Figures 4(c)–(d) that when the newly added DSIRs (Rc1, Rd1) were placed in the proper position, the existing external quality factors were weakly affected by the newly added DSIRs. Based on this feature, the external quality factors ($Qe1$, $Qe2$, $Qe3$, and $Qe4$) between the input resonators and common feeding line can be extracted and quantified from Figures 4(a)–(d).

When the input external quality factors are determined, the other parts of the quadruplexer can be easily determined making use of classical single filter design theory. The extracting of coupling coefficient of a pair of DSIRs is much similar to that of SIRs. The computation equation of coupling coefficients by simulation are given by [24],

$$M_{ij} = \frac{f_{p1}^2 - f_{p2}^2}{f_{p1}^2 + f_{p2}^2} \tag{2}$$

where M_{ij} represents the coupling coefficient between resonators i and j, f_{p1} and f_{p2} are defined to be the lower and higher of the two resonant frequencies, respectively.

According to the orientation of two folded DSIRs, the coupling can be electric, magnetic and mixed as shown in Figures 5(a)–(c). Because DSIR has an opposite electromagnetic field distribution to the microstrip SIR, its coupling property is also different from SIR. For example, the structure shown in Figure 5(a) takes on electric coupling for DSIRs but magnetic coupling for SIRs, while Figure 5(b) depicts the inverse case and Figure 5(c) shows the mixed coupling case. Given a coupling coefficient M_{ij} between two adjacent resonators, the physical control parameters are the coupling gap (g) and the displacement (h). Obviously, a smaller coupling gap or displacement will result in larger coupling coefficients for all of the channels.

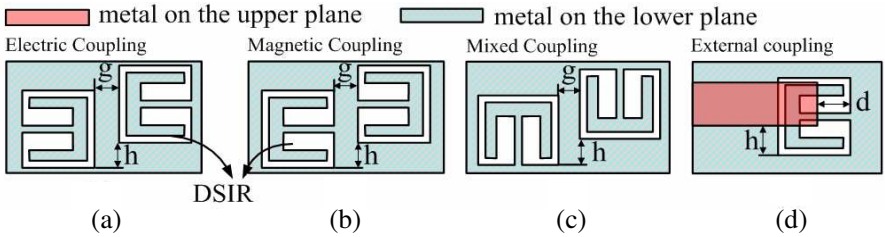

Figure 5. Internal and output external coupling structures with DSIRs. (a) Electric coupling. (b) Magnetic coupling. (c) Mixed coupling. (d) Output external coupling.

The output external coupling of the DSIR is also realized by parallel microstrip feeding line. Different from the SIR, the DSIR may have an overlapped part with the microstrip feeding line to achieve a large enough coupling strength. Figure 5(d) illustrates the external coupling structure of DSIR with an overlapped feeding line, where the feeding line is parallel to the split-ring edge of the output resonator and has an inserted distance (d) and displacement (h). Once the d and the h are given, the external coupling coefficient of the DSIR, which increases evidently with the increase of inserted distance and displacement, can be determined easily.

Based on the foregoing analysis of the coupling structures, the design procedure for the proposed quadruplexer is summarized as follows:

1) According to the quadruplexer specification, independently synthesize the values of coupling coefficients and external quality factors for each channel filter.
2) Fixing the impedance ratio value and the length of the parallel side, determine the physical dimensions of the DSIRs which will be used in the four channels.
3) Determine the inserted distance ($L1$, $L2$ and $L3$) and displacement ($D1$, $D2$, $D3$ and $D4$) of the input DSIRs to satisfy the input external couplings. Though there are many cases satisfying the specifications, one should pay attention to the selection of the inserted distance and the displacement as the resonators of different channels might overlap.
4) Extract the coupling gap and the displacement together according to the coupling coefficients, and corresponding physical parameters of the output feeding lines by the output external quality factors, then obtain the size of the four channels, respectively.

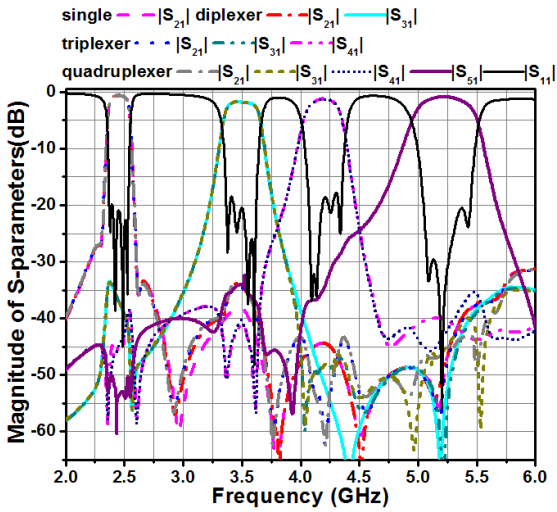

Figure 6. Simulated S parameters of a single-band BPF, diplexer, triplexer and quadruplexer.

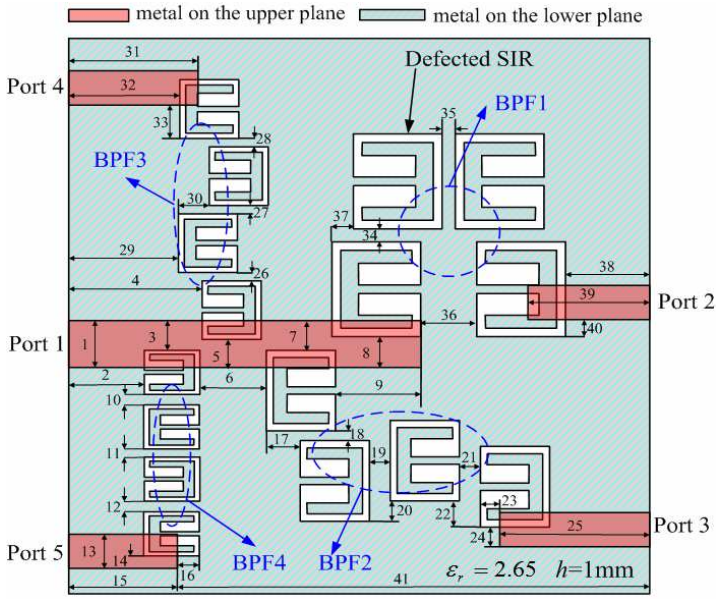

Figure 7. Layout of the proposed quadruplexer.

5) Combine the four channels into a quadruplexer by sharing the common input feeding line. It should be noted that the loading effect among channels is very small, which can be seen in Figure 6 where the simulated results of a single-band bandpass filter (2.45 GHz), a diplexer (2.45 and 3.5 GHz), a triplexer (2.45, 3.5, and 4.2 GHz), and a quadruplexer (2.45, 3.5, 4.2, and 5.25 GHz) are illustrated. From the single-band bandpass filter fixed at the upper right to the quadruplexer as shown in Figure 7, the channels are constructed one by one clockwise. For example, the only difference between the quadruplexer and the triplexer is the added three resonators and output feeding line at port 5 for the fourth channel. The loading effect is negligible since the newly added resonators have little effect on the existing channels.

Figure 7 describes the layout of the proposed quadruplexer. After an optimization process by using Zeland IE3D software, the final dimensions of the designed quadruplexer are obtained as shown in Table 3.

Table 3. Optimal dimensions (in mm) of each part of the quadruplexer (Figure 7).

Part Number	1	2	3	4	5	6
Dimension	3.3	7.9	1.3	14.0	1.27	9.0
Part Number	12	13	14	15	16	17
Dimension	0.7	2.7	1.4	11.9	0.42	3.3
Part Number	23	24	25	26	27	28
Dimension	0.15	1.4	13.65	0.55	1.45	1.2
Part Number	34	35	36	37	38	39
Dimension	1.35	0.7	6.9	2.2	7.5	10.55
Part Number	7	8	9	10	11	-
Dimension	2.2	2.1	4.45	0.45	0.95	-
Part Number	18	19	20	21	22	-
Dimension	0.9	1.15	2.15	1.85	1	-
Part Number	29	30	31	32	33	-
Dimension	10.85	3.5	13.65	10.85	3.73	-
Part Number	40	41				-
Dimension	1.33	41.75				-

4. RESULTS AND DISCUSSION

With the geometric parameters listed above, a microstrip filter is fabricated on the substrate with relative dielectric of 2.65 and height of 1 mm, and measured using Agilent's 8719ES network analyzer. A photograph of a fabricated circuit is presented in Figure 8. The circuit size of the proposed quadruplexer is $53\,\text{mm} \times 58\,\text{mm} = 0.64\lambda_g \times 0.70\lambda_g$, where λ_g is the guided wavelength of 50-line on the substrate at the center frequency (2.45 GHz) of the first channel.

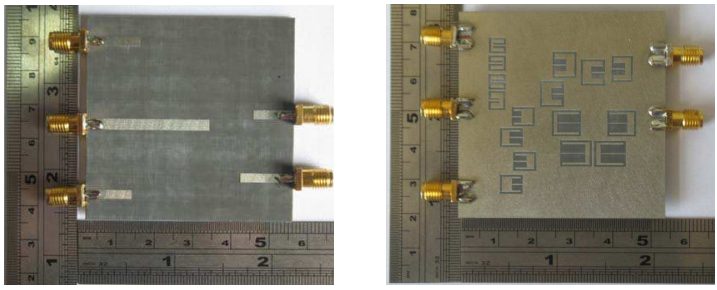

(a) (b)

Figure 8. Photograph of the fabricated quadruplexer. (a) Top view. (b) Bottom view.

The simulated and measured results of the fabricated quadruplexer are shown together in Figure 9. It's can be seen from this figure that the measured results are in good agreements with the simulated ones. The simulated results are centered at 2.45/3.5/4.2/5.25 GHz, with fractional bandwidths of 6.5%, 7.0%, 6.6% and 7.5%, respectively. In the measurements, the four channels are centered at 2.44/3.52/4.19/5.24 GHz, with the fractional bandwidths of 5.9%, 6.5%, 6.0% and 7.1%, respectively. The measured insertion loss at the channel center frequencies are 2.3 dB, 2.6 dB, 2.5 dB, and 2.5 dB, respectively and the return loss of the quadruplexer has reached larger than 15 dB. The measured isolations amongst channels were over 35 dB as shown in Figure 9(c). Due to the dielectric loss and radiation loss, the experimental insertion loss is larger than the analytical results by about 0.8 dB. This planar quadruplexer can be placed inside a conductive enclosure with four metal posts at each corner of the ground to reduce the radiation loss.

Based on the results presented in this study, it should be mentioned that the proposed configuration has the potential to be

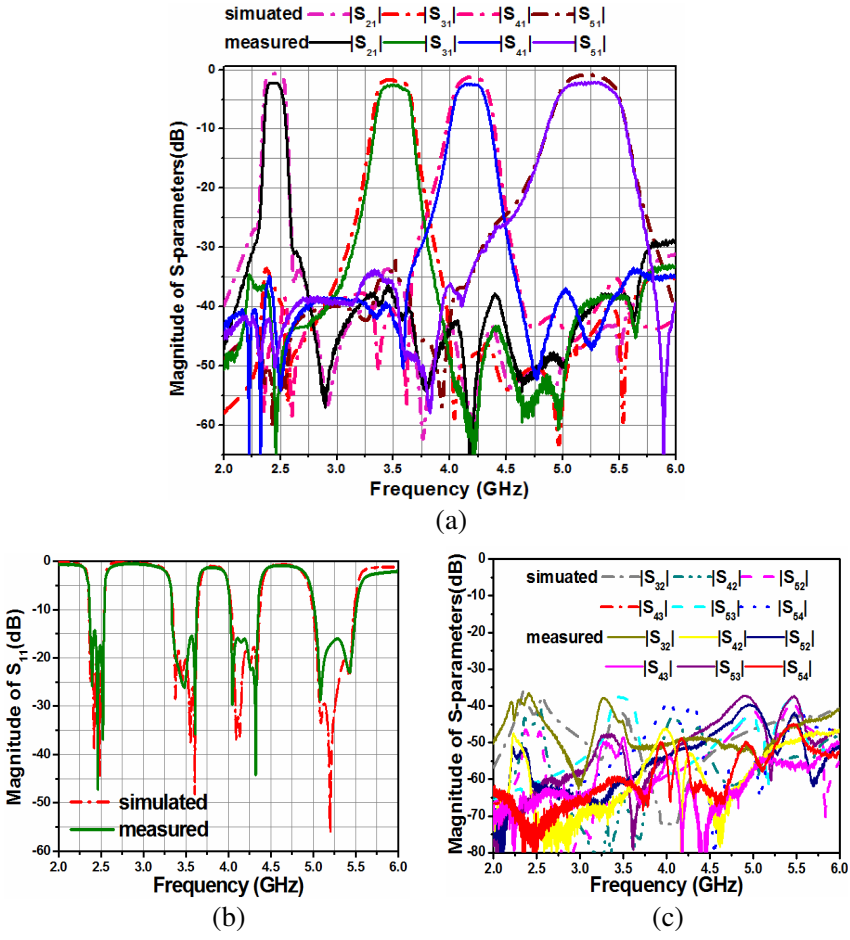

Figure 9. Simulated and measured response of the fabricated quadruplexer. (a) Transmission characteristic. (b) Reflection characteristic. (c) Isolation characteristic.

applied to multiplexer design with even more channels. Unlike the multiplexers using common resonators that have limited passband numbers due to the small coupling area, the microstrip feeding line can accommodate many passbands based on DSIRs. Furthermore, the ones using common resonators have limited freedom in passband frequency selection as the frequency should be the same as the resonator's resonant frequency.

5. CONCLUSION

In this study, a compact and high-isolation quadruplexer with arbitrary passband frequencies is presented. The detailed design procedure is given. By locating the input DSIRs of each channel properly, the loading effect among the four channels is negligible, so that the implementation of a quadruplexer becomes convenient. In addition, the proposed configuration is ready to be applied in multiplexers with more channels. The above features make the proposed scheme attractive in multiplexer design. The measurements of the fabricated component confirm that the quadruplexer is characterized by a compact size, good band performance, and selectivity comparable to that of the prototype.

ACKNOWLEDGMENT

This work was supported by the National Natural Science Foundation of China (NSFC) under project No. 60901030, No. 60901031 and No. 72005477.

REFERENCES

1. Lin, Y.-S., C.-C. Liu, K.-M. Li, and C.-H. Chen, "Design of an LTCC tri-band transceiver module for GPRS mobile applications," *IEEE Trans. Microwave Theory Tech.*, Vol. 52, 2718–2724, 2004.
2. Jimenez Martin, J. L., V. Gonzalez-Posadas, J. E. Gonzalez-Garcia, F. J. Arques-Orobon, L. E. Garcia-Munoz, and D. Segovia-Vargas, "Dual band high efficiency class ce power amplifier based on CRLH diplexer," *Progress In Electromagnetics Research*, Vol. 97, 217–240, 2009.
3. Zewani, M. and I. C. Hunter, "Design of ring-manifold microwave multiplexers," *IEEE MTT-S Int. Dig.*, 689–692, San Francisco, CA, Jun. 2006.
4. Deng, P.-H., N.-I. Lai, S.-K. Jeng, and C. H. Chen, "Design of matching circuits for microstrip triplexers based on stepped-impedance resonators," *IEEE Trans. Microwave Theory Tech.*, Vol. 54, 4185–4192, 2006.
5. Shi, J., J.-X. Chen, and Z.-H. Bao, "Diplexers based on microstrip line resonators with loaded elements," *Progress In Electromagnetics Research*, Vol. 115, 423–439, 2011.

6. Yao, W. H., A. E. Abdelmonem, J. F. Liang, X. P. Liang, K. A. Zaki, and A. Martin, "Wide-band waveguide and ridge waveguide T-junctions for diplexer applications," *IEEE Trans. Microwave Theory Tech.*, Vol. 41, 2166–2173, 1993.
7. Han, S., X.-L. Wang, Y. Fan, Z. Yang, and Z. He, "The generalized Chebyshev substrate integrated waveguide diplexer," *Progress In Electromagnetics Research*, Vol. 73, 29–38, 2007.
8. Chen, X.-W., W.-M. Zhang, and C.-H. Yao, "Design of microstrip diplexer with wide band-stop," *International Conference on Microwave and Millimeter Wave Technology*, 1–3, 2007.
9. Yang, R.-Y., C.-M. Hsiung, C.-Y. Hung, and C.-C. Lin, "Design of a high band isolation diplexer for GPS and WLAN system using modified Stepped-Impedance Resonators," *Progress In Electromagnetics Research*, Vol. 107, 101–114, 2010.
10. He, Z. R., X. Q. Lin, and Y. Fan, "Improved stepped-impedance resonator (SIR) bandpass filter in Ka-band," *Journal of Electromagnetic Waves and Applications*, Vol. 23, No. 8–9, 1181–1190, 2009.
11. Yang, M. H., J. Xu, Q. Zhao, and X. Sun, "Wide-stopband and miniaturized lowpass filters using SIRs-loaded hairpin resonators," *Journal of Electromagnetic Waves and Applications,* Vol. 23, No. 17–18, 2385–2396, 2009.
12. Yang, R.-Y., C.-M. Hsiung, C.-Y. Hung, and C.-C. Lin, "A high performance bandpass filter with a wide and deep stopband by using square stepped impedance resonators," *Journal of Electromagnetic Waves and Applications*, Vol. 24, Nos. 11–12, 1673–1683, 2010.
13. Yu, W.-H., J.-C. Mou, X. Li, and X. Lv, "A compact filter with sharp-transition and wideband-rejection using the novel defected ground structure," *Journal of Electromagnetic Waves and Applications*, Vol. 23, No. 2–3, 329–340, 2009.
14. Guo, Y. C., L. H. Weng, and X. W. Shi, "An improved microstrip open loop resonator bandpass filter with DGSS for WLAN application," *Journal of Electromagnetic Waves and Applications*, Vol. 23, No. 4, 463–472, 2009.
15. Huang, C.-Y., M.-H. Weng, C.-S. Ye, and Y.-X. Xu, "A high band isolation and wide stopband diplexer using dual-mode stepped-impedance resonators," *Progress In Electromagnetics Research*, Vol. 100, 299–308, 2010.
16. Deng, P. H., C. H. Wang, and C. H. Chen, "Compact microstrip diplexers based on a dual-passband filter," *Proceedings of Asia-Pacific Microwave Conference*, 2006.

17. Wu, H.-W., K. Shu, M.-H. Weng, J.-R. Chen, and Y.-K. Su, "Design of a compact microstrip triplexer for multiband applications," *Proc. Eur. Microw. Conf.*, 834–837, 2007.
18. Chen, C.-F., T.-Y. Huang, T.-M. Shen, and R.-B. Wu, "A miniaturized microstrip common resonator triplexer without extra matching network," *Proc. Asia-Pacific Microw. Conf.*, 1439–1442, 2006.
19. Chen, C.-F., T.-Y. Huang, C.-P. Chou, and R.-B. Wu, "Microstrip diplexer design with common resonator section for compact size but high isolation," *IEEE Trans. Microwave Theory Tech.*, Vol. 54, 1945–1952, 2006.
20. Amari, S., "Synthesis of cross-coupled resonator filters using an analytical gradiant-based optimization technique," *IEEE Trans. Microwave Theory Tech.*, Vol. 9, 1559–1564, 2000.
21. Huang, J.-Q., Q.-X. Chu, and C.-Y. Liu, "Compact UWB filter based on surface-coupled structure with dual notched bands," *Progress In Electromagnetics Research*, Vol. 106, 311–319, 2010.
22. Wei, F., L. Chen, Q.-Y. Wu, X.-W. Shi, and C.-J. Gao, "Compact UWB bandpass filter with narrow notch-band and wide stop-band," *Journal of Electromagnetic Waves and Applications*, Vol. 24, No. 7, 911–920, 2010.
23. Hsiao, P.-Y. and R.-M. Weng, "Compact open-loop UWB filter with notched band," *Progress In Electromagnetics Research Letters*, Vol. 7, 149–159, 2009.
24. Hong, J.-S. and M. J. Lancaster, *Microstrip Filter for F/Microwave Applications*, Wiley, New York, 2001.